Physics (Cornell Univ. Press, Ithaca, NY, 1979); F. W. Wiegel, *Conformational Phase Transitions in a Macromolecule: Exactly Solvable Models in Phase Transitions and Critical Phenomena*, C. Domb and J. L. Lebowitz, Eds. (Academic Press, New York, 1983), vol. 7.
4. F. S. Bates and G. H. Fredrickson, *Annu. Rev. Phys. Chem*. **41**, 525 (1990).
5. For a discussion of several of the processes leading to self-organization, see special issue on the 1996 NATO Workshop on Tandem Molecular Interactions, in R. Zentel, G. Galli, C. K. Ober, Eds., *Macromol. Symp*. **117** (1997).
6. E. Dessipri, D. A. Tirrell, E. D. T. Atkins, *Macromolecules* **29**, 3545 (1996).
7. M. Muthukumar, *J. Chem. Phys*. **103**, 4723 (1995); *Comput. Mater. Sci.* **4**, 370 (1995).
8. For the specific example of diblock copolymers, the topological connectivity of various monomers in every chain appears as a density-density correlation at a distance r being proportional to $1/r$ so that $\alpha = 2$ (the Fourier transform of $1/r$ is $1/k^2$ in three dimensions). The long-range interaction can originate from such entropic correlations or electrostatic interactions (as in the case of surfactant and polyelectrolyte solutions) or chemical reactions (as in the case of simultaneous occurrence of macrophase separation and chemical reactions or hydrogen bonding).
9. The scheme requires consideration of shape and packing at the atomic and molecular level as well as at higher levels of scale leading to the three dimensional structure of the overall aggregate. Bringing the set of components together into the requisite array in a single process step (for example, by cooling the mixture) is extremely difficult, particularly when the basic units have conformational diversity under the conditions of the assembly process. Indeed, this situation is a critical issue, for if the system or parents of the system adopt wrong shapes and packings, then the desired structures may not even form.
10. A. H. Simmons, C. A. Michal, L. W. Jelinski, *Science* **271**, 84 (1996).
11. T. Gulik-Krzywicki, C. Fouquey, J.-M. Lehn, *Proc. Natl. Acad. Sci. U.S.A.* **90**, 163 (1993); M. Kotera, J.-M. Lehn, J.-P. Vigneron, *Tetrahedron* **51** (No. 7), 1953 (1995).
12. M. Müller, F. Kremer, R. Stadler, E. W. Fischer, U. Seidel, *Colloid Polym. Sci.* **273**, 38 (1995).
13. T. Kato, H. Kihara, U. Kumar, T. Uryu, J. M. J. Fréchet, *Angew. Chem. Int. Ed. Engl.* **33**, 1644 (1994); T. Kato, M. Nakano, T. Moteki, T. Uryu, S. Ujiie, *Macromolecules* **28**, 8875 (1995).
14. C. G. Bazuin, F. A. Brandys, T. M. Eve, M. Plante, *Macromol. Symp.* **84**, 183 (1994); C. G. Bazuin and A. Tork, *Macromolecules* **28**, 8877 (1995); R. Tal'roze, S. Kuptsov, T. Sycheva, V. Bezborodov, N. Plate, *ibid.*, p. 8689.
15. J. Ruokalainen *et al*., *Macromolecules* **28**, 7779 (1995); J. Ruokalainen, G. ten Brinke, O. Ikkala, M. Torkkeli, R. Serimaa, *ibid.* **29**, 3409 (1996).
16. A. Pron, J. Lostra, J.-E. Österholm, P. J. Smith, *Polymer* **34,** 4235 (1993); T. Vikki *et al*., *Macromolecules* **29**, 2945 (1996).
17. Peter R. Ashton *et al*., *Angew. Int. Ed. Engl*. **36**, 735 (1997).
18. C. Gong and H. Gibson, *Macromolecules* **29**, 7029 (1996); G. Wenz, *Angew. Chem. Int. Ed. Engl.* **33**, 803 (1994).
19. C. K. Ober and G. Wegner, *Adv. Mater*. **9**, 17 (1997).
20. V. Percec and G. Johansson, *Macromol. Symp.* **95**, 173 (1995).
21. J. M. Park, B. B. Muhoberac, P. L. Dubin, J. Xia, *Macromolecules* **25**, 290 (1992).
22. E. L. Thomas, D. M. Anderson, C. J. Henkee, D. Hoffman, *Nature* **334**, 598 (1988).
23. J. M. Seddon, *Biochim. Biophys. Acta* **1031**, 1 (1990); T. Hashimoto, M. Takenaka, T. Izumitani, *J. Chem. Phys.* **97**, 697 (1992); J. Lauger, R. Lay, W. Gronski, *ibid.* **101**, 7181 (1994).
24. J.-P. Billot, A. Douy, B. Gallot, *Makromol. Chem*. **178**, 1641 (1977).
25. J. Adams and W. Gronski, *Makromol. Chem. Rapid Commun*. **10**, 553 (1989).
26. S. I. Stupp *et al*., *Science* **276**, 384 (1997).
27. J. T. Chen, E. L. Thomas, C. K. Ober, G.-P. Mao, *ibid.* **273**, 343 (1996); J. T. Chen *et al.*, *Macromolecules* **28**, 1688 (1995).
28. G.-P. Mao *et al*., *Macromolecules* **30**, 2556 (1997).
29. A. Omenat, R. A. M. Hikmet, J. Lub, P. Van der Sluis, *ibid.* **29**, 6730 (1996); W. Y. Zheng and P. T. Hammond, *Macromol. Rapid Commun.* **17**, 813 (1996).
30. M. Brehmer, R. Zentel, G. Mao, C. K. Ober, *Macromol. Symp.* **117**, 245 (1997).
31. J.-G. Wang, G.-P. Mao, C. K. Ober, E. J. Kramer, *Macromolecules* **30**, 1906 (1997).
32. We have benefited from interactions with many students and co-workers and would like to thank former members of our research groups. In particular, C.K.O. thanks G.-P. Mao and J.-G. Wang and E.L.T. thanks J. T. Chen. Funding from NSF (DMR-970527) (to M.M., C.K.O., and E.L.T.) and both NSF (DMR-9201845) and the Air Force Office of Sponsored Research (MURI PC 218975) (to C.K.O. and E.L.T.) is gratefully acknowledged. C.K.O. thanks the Office of Naval Research for support of the fluoropolymer work.

Fuzzy Nanoassemblies: Toward Layered Polymeric Multicomposites

Gero Decher

Multilayer films of organic compounds on solid surfaces have been studied for more than 60 years because they allow fabrication of multicomposite molecular assemblies of tailored architecture. However, both the Langmuir-Blodgett technique and chemisorption from solution can be used only with certain classes of molecules. An alternative approach—fabrication of multilayers by consecutive adsorption of polyanions and polycations—is far more general and has been extended to other materials such as proteins or colloids. Because polymers are typically flexible molecules, the resulting superlattice architectures are somewhat fuzzy structures, but the absence of crystallinity in these films is expected to be beneficial for many potential applications.

In the last two to three decades, materials science has developed into an interdisciplinary field that encompasses organic, polymeric, and even biological components in addition to the classic metals and inorganics. Although carbon-based molecules offer an enormous structural diversity and tunability in terms of potential properties or processability, they also typically suffer from a lack of stability when exposed to heat, oxidizing agents, electromagnetic radiation, or (as in the case of complex biomolecules) dehydration. Multicomposites make it possible to combine two or more desirable properties, as in the classic reinforced plastics, or to provide additional stability for otherwise highly labile functional biomolecules or biomolecular assemblies. Even higher device functionality will arise from a combination of physical and chemical processes (such as electron or energy transfer) and chemical transformations found in nature (such as photochemical energy conversion). Such devices require control of molecular orientation and organization on the nanoscale, as their function strongly depends on the local chemical environment. It is therefore highly desirable to develop methods for the controlled assembly of multicomponent nanostructures, although it is also clear that structures as complex as those found in the biological world, such as the flagellar motor, cannot yet be fabricated.

It is, however, possible to consecutively deposit single molecular layers onto planar solid supports and to form multilayers in which nanoscale arrangements of organic molecules can be controlled at least in one dimension (along the layer normal). This approach also fulfills another prerequisite for functional macroscopic devices: a fixed relation between nanoscopic order and macroscopic orientation. To fully exploit an assembled structure, it is necessary to know the location or orientation (or both) of every molecule, not only with respect to each other (as in ordered or phase-separated bulk systems at the nanometer scale, such as liquid crystals, copolymers, or zeolites), but also with respect to a macroscopic coordinate. Only materials that have such structural hierarchy (*1*) allow molecular properties to be fully exploited in macroscopic devices, as, for example, in organic waveguides for second-order nonlinear optics or in biosensors.

In simple multilayer systems, this demand is reduced to the sequence of layers and to the orientation of molecules with respect to the layer normal. For about 60 years, the molecularly controlled fabrica-

Université Louis Pasteur and CNRS, Institut Charles Sadron, 6, rue Boussingault, F-67083 Strasbourg Cedex, France. E-mail: decher@ics-crm.u-strasbg.fr

tion of nanostructured films has been dominated by the so-called Langmuir-Blodgett (LB) technique, in which monolayers are formed on a water surface and then transferred onto a solid support (*2*, *3*). Indeed, the pioneering work on synthetic nanoscale heterostructures of organic molecules was carried out by Kuhn and co-workers in the late 1960s using the LB technique (*4*). Their experiments with donor and acceptor dyes in different layers of LB films provided direct proof of distance-dependent Förster energy transfer on the nanoscale. These experiments were also the first true nanomanipulations, as they allowed for the mechanical handling of individual molecular layers (such as separation and contact formation) with angstrom precision (*5*).

The LB technique requires special equipment and has severe limitations with respect to substrate size and topology as well as film quality and stability. Since the early 1980s, self-assembly techniques based mainly on silane-SiO_2 (*6*) and metal phosphonate chemistry (*7*) were developed as an alternative to LB films. However, self-assembled films based on covalent or coordination chemistry are restricted to certain classes of organics, and high-quality multilayer films cannot be reliably obtained. These problems are most likely caused by the high steric demand of covalent chemistry and the severely limited number of reactions with exactly 100% yield, which is a prerequisite for the preservation of functional group density in each layer.

It was therefore desirable to develop a simple approach that would yield nanoarchitecture films with good positioning of individual layers, but whose fabrication would be largely independent on the nature, size, and topology of the substrate. The electrostatic attraction between oppositely charged molecules seemed to be a good candidate as a driving force for multilayer buildup, because it has the least steric demand of all chemical bonds. Since the early 1990s, our group has developed a technique for the construction of multicomposite films of rodlike molecules equipped with ionic groups at both ends (*8*), polyelectrolytes (*9*), or other charged materials through layer-by-layer adsorption from aqueous solution (*10*, *11*). The process, which is extremely simple, is depicted in Fig. 1 for the case of polyanion-polycation deposition on a positively charged surface. Strong electrostatic attraction occurs between a charged surface and an oppositely charged molecule in solution; this phenomenon has long been known to be a factor in the adsorption of small organics and polyelectrolytes (*12*), but it has rarely been studied with respect to the molecular details of layer formation (*13*). In principle, the adsorption of molecules carrying more than one equal charge allows for charge reversal on the surface, which has two important consequences: (i) repulsion of equally charged molecules and thus self-regulation of the adsorption and restriction to a single layer, and (ii) the ability of an oppositely charged molecule to be adsorbed in a second step on top of the first one. Cyclic repetition of both adsorption steps leads to the formation of multilayer structures.

The crucial factor of charge reversal of a surface upon adsorption of an oppositely charged polyelectrolyte has long been known for the case of polyion adsorption on colloids, but has also been observed on macroscopic surfaces (*14*, *15*). The consecutive adsorption of cationic colloids composed of a heparin-hexadecylamine complex and of pure heparin on polyethylene surfaces that were oxidized or sulfated (or both) leads to films with interesting nonthrombogenic properties (*16*). However, these films were reported to be homogeneous monolayers that arise from submonolayer coverage after the first deposition cycle and subsequent completion of surface coverage in cycles 2 to 5; additional deposition cycles lead to surface flocculation and destruction of layer uniformity. This report was rather discouraging given the early and promising experiments of Iler on the fabrication of multilayers of charged inorganic colloids by consecutive adsorption (*17*), which were never proven to be layered structures or the protein-polyelectrolyte multilayers proposed by Fromherz in 1980 (*18*).

Sequential cationic-anionic polyelectrolyte addition has important consequences for flocculation and is therefore of interest in large-scale industrial processes such as sewage dewatering or paper making, and the two-step treatment of colloids or cellulosic fibers with polycations and polyanions has been studied for many years (*19*, *20*). However, the process is considered difficult and the resulting structures are not well understood; therefore, existing industrial applications may benefit from a better understanding of polyelectrolyte multilayer films as model systems, as these can be well characterized by a wide variety of physical techniques.

Fabrication of Polyelectrolyte and Related Multilayers

Multilayer structures composed of polyions or other charged molecular or colloidal objects (or both) are fabricated as schematically outlined in Fig. 1. Because the process only involves adsorption from solution, there are in principle no restrictions with respect to substrate size and topology; multilayers have been prepared on colloids and on objects with dimensions of several tens of centimeters. Film deposition on a glass slide from ordinary beakers can be carried out either manually or by an automated device (*21*) (Fig. 1A). A representation of the buildup of a multilayer film at the molecular level (Fig. 1B) shows a positively charged substrate adsorbing a polyanion and a polycation consecutively; in this example, the counterions have been omitted

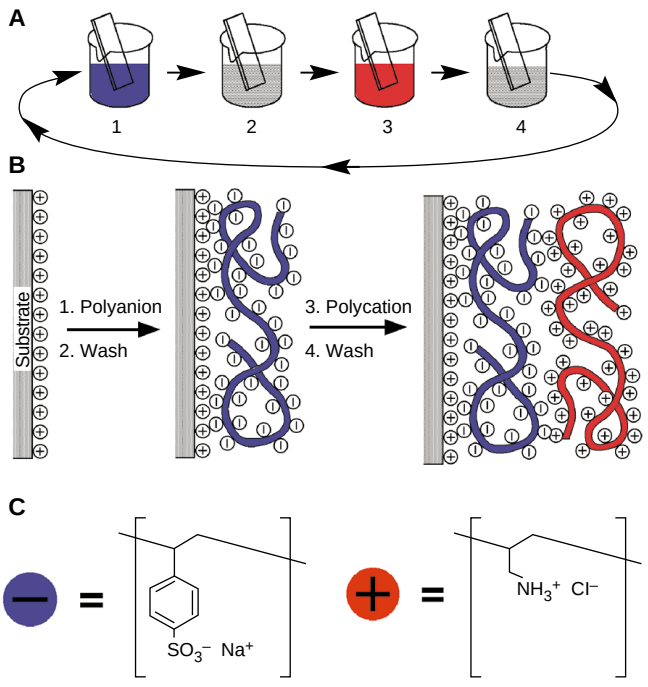

Fig. 1. (**A**) Schematic of the film deposition process using slides and beakers. Steps 1 and 3 represent the adsorption of a polyanion and polycation, respectively, and steps 2 and 4 are washing steps. The four steps are the basic buildup sequence for the simplest film architecture, $(A/B)_n$. The construction of more complex film architectures requires only additional beakers and a different deposition sequence. (**B**) Simplified molecular picture of the first two adsorption steps, depicting film deposition starting with a positively charged substrate. Counterions are omitted for clarity. The polyion conformation and layer interpenetration are an idealization of the surface charge reversal with each adsorption step. (**C**) Chemical structures of two typical polyions, the sodium salt of poly(styrene sulfonate) and poly(allylamine hydrochloride).

and the stoichiometry of charged groups between polyions and between the substrate and polyanion is arbitrary (see below). Two typical polyelectrolytes, sodium poly(styrene sulfonate) and poly(allylamine hydrochloride), are shown in Fig. 1C.

The use of polyelectrolytes rather than small molecules is advantageous mainly because good adhesion of a layer to the underlying substrate or film requires a certain number of ionic bonds. Therefore, the overcompensation of the surface charge by the incoming layer is more a property of the polymer than a property of the surface. This is because polymers can simply bridge over underlying defects; their conformation at the surface (and thus also the newly created film surface) is mostly dependent on the chosen polyelectrolytes and adsorption conditions and much less dependent on the substrate or the substrate charge density (*10*, *22*). The linear increase of film thickness with the number of deposited layers is often similar even if different substrates are used, which makes the film properties rather independent of the substrate. In cases where substrate charge densities are very small, the first layer binds to the surface with only a few groups and exposes a larger number of oppositely charged groups to the solution. This effective "multiplication of surface functionality" often continues over a few layers before a linear deposition regime is reached (*22*–*26*).

Similar to this self-regulation of thickness increments per layer, there is a tendency toward a certain value of the interfacial overlap between a polyanion layer and a polycation layer and a certain roughness at the film-air interface; these attributes are probably a property of the polyanion-polycation pair rather than a property of the substrate. We have observed that polyelectrolyte multilayers have similar surface roughness, regardless of the roughness of the underlying substrates. One possible explanation is that the surface roughness of rough polyelectrolyte films can be "annealed" to smaller values by consecutively immersing films in solutions of salt and pure water (*27*). Presumably, in this post-preparation treatment of the films, the salt breaks some of the anion-cation bonds, and its removal by washing in pure water leads to their reformation in a more equilibrated conformation of the polymer chains.

Films are typically deposited from adsorbate concentrations of several milligrams per milliliter. These concentrations are much greater than that required to reach the plateau of the adsorption isotherm, but this excess ensures that the solutions do not become depleted during the fabrication of films composed of several hundred layers. One or more washing steps are usually used after the adsorption of each layer to avoid contamination of the next adsorption solution by liquid adhering to the substrate from the previous adsorption step. The washing step also helps to stabilize weakly adsorbed polymer layers (*24*). Typical adsorption times per layer range from minutes in the case of polyelectrolytes (*24*, *25*, *28*) to hours in the case of gold colloids (*29*, *30*), depending on molar masses, concentrations, and agitation of the solutions.

The major advantages of layer-by-layer adsorption from solution are that many different materials can be incorporated in individual multilayer films and that the film architectures are completely determined by

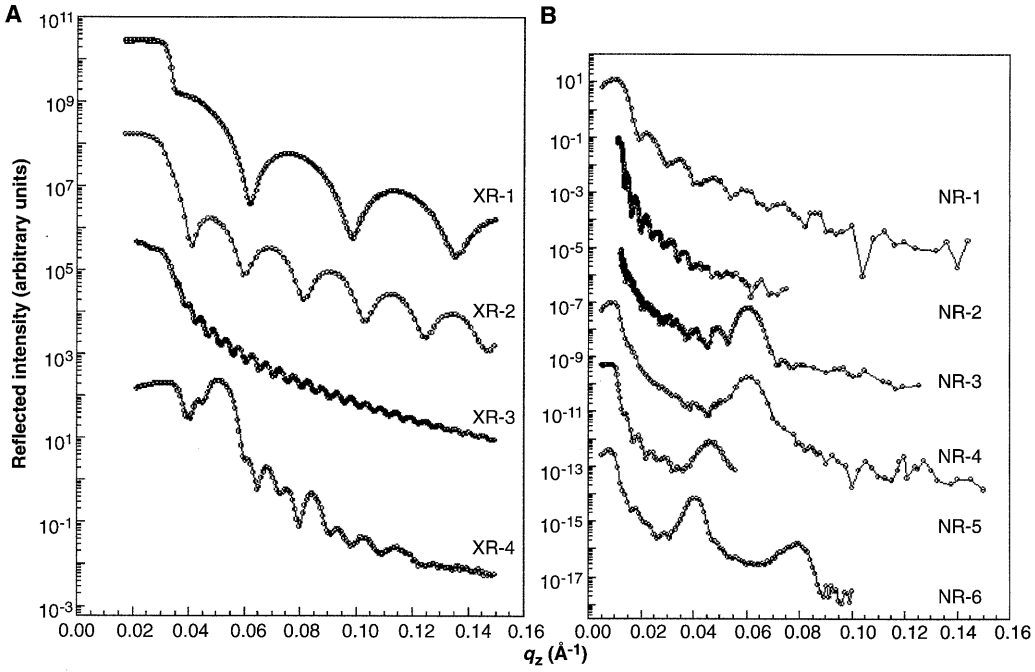

Fig. 2. (**A**) Curves XR-1, XR-2, and XR-3 are specular x-ray reflectivity scans of multilayer films composed of poly(styrene sulfonate) and poly(allylamine hydrochloride). Only partial curves for XR-1 and XR-2 are shown, to keep the same range of the scattering vector q for all scans and for better comparison with (B). The film thicknesses increase from 16.5 nm to 120.5 nm because of different numbers of layers and deposition from solution containing different amounts of salt. All curves can be modeled quantitatively with a film of homogeneous thickness and no internal structure. Scan XR-3 was taken from the same film specimen as curve NR-6 in (B); however, its internal layer structure is only detected by neutron reflectivity. XR-4 is a reflectivity scan of a multilayer with the architecture $((A/B)_3A/G)_4$, where G consists of negatively charged gold colloids of 13.5 nm diameter (*30*). The superlattice formed by the layers of the gold colloids is clearly seen; the high intensity of the (001) Bragg peak arises from the large electron density difference between the polymers and the gold. Scans are shifted in the y direction to preserve clarity. (**B**) Curves NR-1 to NR-6 are specular neutron reflectivity scans of multilayer films; all except NR-5 were obtained from films composed of sodium poly(styrene sulfonate) and poly(allylamine). NR-1 and NR-2 are scans of films in which every second layer was deuterated $[(A/B_d)_n$ film architecture]. NR-3 has an $(A/B/A/B_d)_n$ architecture and was measured from the same film specimen as NR-4 after 11 months of storage in a regular laboratory, demonstrating the good stability of multilayer films over time. Scan NR-6 has $((A/B)_2A/B_d)_n$ architecture and was measured from the same specimen that does not show Bragg peaks in x-ray reflectivity [(A), scan XR-3]. Although different in architecture, the positions of the deuterated layers in samples NR-2 and NR-3 were approximately matched by depositing NR-2 from 3 M NaCl and NR-3 from 2 M NaCl; therefore, Bragg peaks, if present, should appear at similar q values. This result rules out the hypothesis that low count rates at high Q values are responsible for the absence of Bragg peaks in NR-1 and NR-2 and shows that the deuteron concentration along the layer normal in $(A/B_d)_n$ films is constant with respect to experimental resolution. NR-5 is a reflectivity scan of a multilayer originally fabricated from poly(styrene sulfonate) and the tetrahydrothiophenium precursor polyelectrolyte of PPV; every fourth poly(styrene sulfonate) layer is perdeuterated. After 32 min of elimination at 120°C, the conversion to PPV is almost complete but the layer structure remains intact, as evidenced from the Bragg peak. Scans are shifted in the y direction to preserve clarity.

the deposition sequence. The most remarkable current examples of multicomposite films include proteins (*31–33*), clay platelets (*31, 34–37*), virus particles (*38*), and gold colloids (*30, 39*). Nanostructured surface-confined films do, of course, have bulk analogs; there are similarities between polyelectrolyte multilayers and their bulk counterparts (*40*). Polyelectrolyte-clay multilayers and bulk organoclay nanocomposites (*41–46*), which have interesting materials properties themselves, may be structurally even closer. However, no straightforward strategy exists to prepare bulk multicomposites with more than two components in which the distance of all constituents or their orientation (or both) can be molecularly controlled. Template approaches such as layer-by-layer assembly are much more promising in this respect. Another difference between bulk systems and surface-confined multilayers is that bulk nanocomposites are often turbid materials, whereas layer-by-layer assembled films can be applied as wavelength-thick transparent coatings on, for example, optical devices.

Structure of Polyelectrolyte Multilayers

Reflectivity techniques, especially neutron and x-ray reflectometry, are well suited for the characterization of multilayer films, as they allow the determination of concentration gradients along the layer normal. In many experiments on multilayer films composed of flexible, strong polyelectrolytes of approximately equal charge-to-charge distances (polyanions and polycations with one charged group per monomer unit), x-ray reflectograms have only exhibited so-called Kiessig fringes that arise from the interference of x-ray beams reflected at the substrate-film and film-air interfaces (*9, 47–49*). Typical reflectivity curves are shown in Fig. 2A (traces XR-1 to XR-3). In these x-ray scans, different numbers of oscillations arise from the different film thicknesses that were obtained either by changing the total number of layers or by depositing from polyelectrolyte solutions of different ionic strength (*10, 47*). They show a large number of well-resolved Kiessig fringes that were originally believed to be caused by the electron densities of two consecutive layers being too close to yield enough contrast. However, neutron reflectograms of films in which all polyanion layers were labeled with deuterium [$(A/B_d)_n$ film architecture, where A is a polycation, B is a polyanion, B_d is a perdeuterated polyanion, and n is the number of deposition cycles] also showed Kiessig fringes as the only characteristic feature (Fig. 2B, traces NR-1 and NR-2). Only when we started to deuterate specific layer positions in a multilayer film were Bragg peaks observed by neutron reflectometry [$((A/B)_mA/B_d)_n$ film architectures, $m = 1, 2, \ldots$; Fig. 2B, traces NR-3 to NR-6], which clearly demonstrated an internal layer structure (*50, 51*). A single Bragg peak was also observed by x-ray reflectivity in films in which every fourth layer was a polyanion containing side groups of azo dyes (*52*). Thus, the absence of Bragg peaks in $(A/B)_n$-type films does not arise from small density differences between different layers, but rather from large overlaps between adjacent layers.

On the basis of this result, together with our inability to detect significant amounts of small counterions in the film, polyelectrolyte multilayers should have a 1:1 stoichiometry of anionic and cationic groups. In this case, every anionic group of a polyanion is bound to a cationic group of a polycation, which is also the predominant case in bulk polyion complexes of flexible polyelectrolytes of high charge density and similar molecular weights (*53*). Note that for weak polyelectrolytes, not all of the monomers need to be charged, so that the overall stoichiometry may deviate from 1:1 (*54*). This has the interesting consequence that within the resolution of the charge-to-charge distance along the polyelectrolyte backbone (typically 0.25 to 0.5 nm), the concentration of anionic and cationic groups must be identical throughout the polyelectrolyte multilayer film and constant along the layer normal. At first, it would seem that such a homogenous distribution of charged ionic groups in the film contradicts the notion of defined individual layers of polyions within such multilayer assemblies, but this apparent discrepancy is easily explained. In a simplified polyelectrolyte multilayer structure composed of 10 layers (Fig. 3), each layer is represented by an arbitrarily chosen sinusoidal concentration profile. The 50% overlap of layers of equal charge has the consequence that at any point inside the film (the substrate-film and film-air interfaces are different), the sum of the concentration of equal ionic groups is unity in both the cationic and anionic case, as represented by the lines composed of blue dots (concentration profile of anionic groups) and red dots (concentration profile of cationic groups). The line composed of green dots represents the concentration profile for a label applied to every fourth layer and shows that chemical functional groups (or labels) can be precisely positioned at certain distances from the substrate or with respect to each other. Thus, Fig. 3 represents a film model in which the high overlap of layers of equal charge allows for a 1:1 stoichiometry of anionic and cationic groups within the film and provides the base for a true layer structure.

The deuterium concentration of such an $(A/B/A/B_d)_n$ film, which is the most important contributor to the scattering length density profile, is described by the line of green dots in Fig. 3. The profile is sinusoidal, which agrees with the observation of a single Bragg peak for this architecture (Fig.

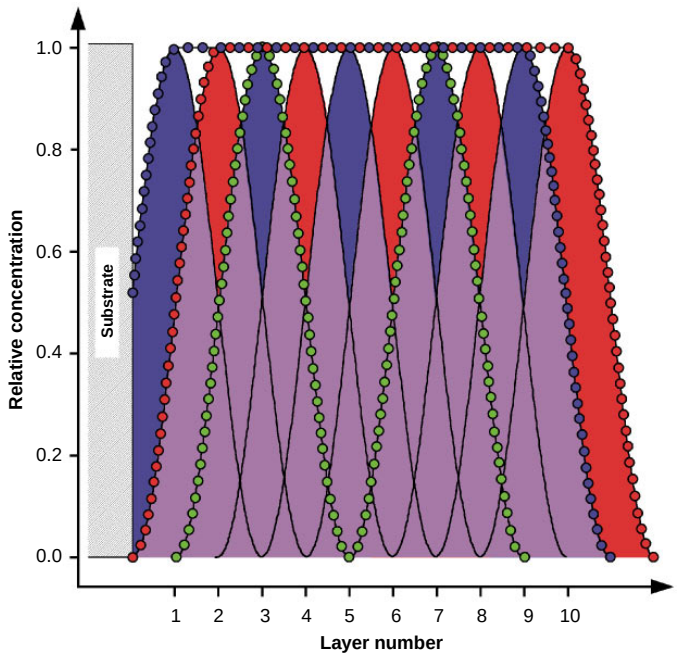

Fig. 3. Schematic of a polyelectrolyte multilayer composed of 10 layers, each represented by an arbitrarily chosen sinusoidal concentration profile (black lines). For a positively charged substrate, the five blue layers and five red layers represent polyanion and polycation layers, respectively. The spread of each layer and the distance between them were chosen such that every two layers of equal charge start to overlap at a relative concentration of 50%. The overlap of blue and red layers (purple) has no physical meaning. The lines composed of blue dots (anionic groups) and red dots (cationic groups) represent the sum of concentrations from all layers within the film. A positional shift of red layers with respect to blue layers causes changes in charge concentration only at the two interfaces, not in the center of the film. The line composed of green dots represents the concentration profile for a label applied to every fourth layer [$(A/B/A/B_d)_n$ architecture = deuterium labels in layers 3 and 7].

2B, scan NR-4). Evaluation of the position of such Bragg peaks has yielded a distance of ~10 nm between the deuterated layers, which depends on the details of film preparation, such as salt concentration in the adsorption solution. If the deuterium labels are placed in every sixth (Fig. 2B, scan NR-6) or eighth layer (concentration profiles not indicated in Fig. 3), the deuterium concentration profile deviates from a sinusoidal curve, and, as a consequence of the anharmonic distortion of the profile, up to four Bragg peaks are observed. These data have been evaluated quantitatively (*55*). Bragg peaks were also observed in films with $(A/B)_n$ architecture (*22, 34, 56*), but in these cases the B layers were composed of inorganic platelets or polymers with stabilized conformations that inhibit overlap with adjacent layers.

The film model as depicted in Fig. 3 is only valid for films composed of simple flexible polyelectrolytes that can form 1:1 complexes. Films composed of more exotic materials will exhibit more complicated structures. A detailed neutron reflectivity study of interfacial roughness differences between poly(styrene sulfonate) and sulfonated poly(aniline) has recently been carried out (*57*).

The apparent macroscopic homogeneity of polyelectrolyte films can actually be an advantage; for example, in optical applications, "fuzzy layered assemblies" do not have any of the defects present in truly crystalline films. This film model of 50% overlap of layers of equal charge also explains the high conductivities found in multilayers composed of conducting polymers (*58*) because the conducting layers are not isolated from each other.

Similar Systems and Potential Applications

The concept of electrostatically driven assembly of multilayer structures allows for the incorporation of a wealth of different materials (*59*). However, polymers as multifunctional materials also offer the choice of building up layered structures through other types of interaction. A biologically interesting interaction is the one between biotin and avidin, and we have used this for the formation of multilayers composed of streptavidin and biotinylated poly(L-lysine) (*60*), which were patterned by photoablation (*61*); similar systems were later used for the electrochemical sensing of glucose (*62*). Polyelectrolyte multilayers have also been fabricated on patterned surfaces (*63–65*). Film deposition is also possible with polymer pairs that can form strong hydrogen-bond bridges (*66*) or by using polymer pairs containing side groups with carbazole and dinitrophenyl units that can form charge-transfer complexes (*67*). Even covalent chemistry can successfully be used for multilayer fabrication, both in purely covalent and in mixed covalent-ionic film architectures using polyamines both as covalent and as ionic layer-forming reagents. Again, the polyfunctionality of the macromolecules makes it possible to avoid the problem of the required 100% yield in every chemisorbed layer, which limits film buildup with small bifunctional organics.

Fullerenes such as C_{60} can be used as covalent building blocks in alternation with polyamines (*68*), because their spherical shape and sixfold reactivity toward amines will always lead to a covalent attachment with the underlying layer (*69*) of polyamine, in which some of the amino-reactive sites of the C_{60} are exposed toward the film surface and thus allow covalent attachment to the next polyamine layer. Another advantage of fullerenes is that they provide scattering length density contrast in neutron reflectivity, and we have shown that covalent multilayers containing C_{60} are true superlattice structures (*70*). However, ionic interactions are the most versatile; they permit the use of water as a solvent, which is both environmentally attractive and allows the use of charged biopolymers such as DNA (*71, 72*) as well as polyelectrolytes, proteins (*31–33, 73*), colloids (*30, 31, 34, 37, 39, 74–77*), and many other charged or chargeable materials.

The incorporation of proteins in multilayer films may lead to the application of polyelectrolyte multilayers as biosensors (*78*) or in biotechnology (*79, 80*); the latter may even provide the base for new developments in multistep chemical catalysis. A crucial point in this type of application will be the control of transport in multilayer films (*72, 81, 82*). Multilayer microcapsules (*83*) may have biomedical applications as well. Multilayer films can also be fabricated on colloids, which may have implications for photovoltaics (*84*). Other possible applications include the incorporation of dye molecules to tailor the optical properties of polyion films (*85–91*). In the case of rodlike amphiphiles carrying hydrophilic head groups at both ends and a central diacetylene group, multilayer systems may also have high in-plane order, because the topochemical polymerization of the diacetylene group only works in a single crystal (*56*).

The use of multilayers as gas separation membranes is a currently developing technology (*92*). As of today, the most advanced development of polyion-based films is probably their potential for the fabrication of light-emitting diodes (*49, 93–103*). This interest was kindled by the demonstration that a water-soluble polyelectrolyte precursor of the intractable electroluminescent polymer poly(*p*-phenylene vinylene) (PPV) can be incorporated into polyelectrolyte films and subsequently thermally converted to PPV (*93*). The neutron reflectivity scan NR-5 in Fig. 2B shows that the multilayer structure of such films, which contain hydrophobic PPV layers after elimination, remains intact (*104*).

Conclusions and Outlook

Layer-by-layer assembly by adsorption from solution is a general approach for the fabrication of multicomponent films on solid supports. Materials can be selected from a pool of small organic molecules, polymers, natural proteins, inorganic clusters, clay particles, and colloids. Although we have only begun to explore useful combinations of materials, the organization of different elementary units in an ordered nanoscopic device may lead to a kind of nanomachinery like that envisioned by Feynman in the 1960s (*105*). One potential property of such devices is a simple dynamic structure in which the distance between two layers of "hard" objects (colloids or proteins) is adjusted by controlling the degree of swelling in an intermediate "soft" layer (polyelectrolyte) simply by changing, for example, humidity. In contrast to bulk systems, where swelling could ruin the mechanical properties of a material, such dynamic structure control could lead to tunable diffraction or optical properties in nanofilm devices.

REFERENCES

1. R. Lakes, *Nature* **361**, 511 (1993).
2. K. B. Blodgett, *J. Am. Chem. Soc.* **56**, 495 (1934).
3. _____ and I. Langmuir, *Phys. Rev.* **51**, 964 (1937).
4. H. Kuhn and D. Möbius, *Angew. Chem. Int. Ed. Engl.* **10**, 620 (1971).
5. O. Inacker, H. Kuhn, D. Möbius, G. Debuch, *Z. Phys. Chem. Neue Folge* **101**, 337 (1976).
6. L. Netzer and J. Sagiv, *J. Am. Chem. Soc.* **105**, 674 (1983).
7. G. Cao, H.-G. Hong, T. E. Mallouk, *Acc. Chem. Res.* **25**, 420 (1992).
8. G. Decher and J.-D. Hong, *Makromol. Chem. Macromol. Symp.* **46**, 321 (1991).
9. _____, J. Schmitt, *Thin Solid Films* **210–211**, 831 (1992).
10. G. Decher, in *Templating, Self-Assembly and Self-Organization*, vol. 9 of *Comprehensive Supramolecular Chemistry*, J.-P. Sauvage and M. W. Hosseini, Eds. (Pergamon, Oxford, 1996), 507–528.
11. W. Knoll, *Curr. Opin. Colloid Interface Sci.* **1**, 137 (1996).
12. M. A. C. Stuart, G. J. Fleer, J. Lyklema, W. Norde, J. M. H. M. Scheutjens, *Adv. Colloid Interface Sci.* **34**, 477 (1991).
13. I. Haller, *J. Am. Chem. Soc.* **100**, 8050 (1978).
14. T. Afsharrad, A. I. Bailey, P. F. Luckham, W. Macnaughton, D. Chapman, *Colloids Surf.* **25**, 263 (1987).
15. P. Berndt, K. Kurihara, T. Kunitake, *Langmuir* **8**, 2486 (1992).
16. C.-G. Gölander, H. Arwin, J. C. Eriksson, I. Lundstrom, R. Larsson, *Colloids Surf.* **5**, 1 (1982).
17. R. K. Iler, *J. Colloid Interface Sci.* **21**, 569 (1966).

18. P. Fromherz, in *Electron Microscopy at Molecular Dimensions*, W. Baumeister and W. Vogell, Eds. (Springer-Verlag, Berlin, 1980), 338–349.
19. H. E. Ries and B. L. Meyers, *J. Appl. Polym. Sci.* **15**, 2023 (1971).
20. R. Aksberg and L. Ödberg, *Nord. Pulp Pap. Res. J.* **5**, 168 (1990).
21. Self-assembly deposition device (Riegler & Kirstein, Wiesbaden, Germany).
22. A. Laschewsky, *Eur. Chem. Chron.* **2**, 13 (1997).
23. Y. M. Lvov and G. Decher, *Crystallogr. Rep.* **39**, 628 (1994).
24. N. G. Hoogeveen, M. A. C. Stuart, G. Fleer, M. R. Böhmer, *Langmuir* **12**, 3675 (1996).
25. R. Advincula, E. Aust, W. Meyer, W. Knoll, *ibid.*, p. 3536.
26. D. Laurent and J. B. Schlenoff, *ibid.* **13**, 1552 (1997).
27. G. B. Sukhorukov, J. Schmitt, G. Decher, *Ber. Bunsenges. Phys. Chem.* **100**, 948 (1996).
28. J. J. Ramsden, Y. M. Lvov, G. Decher, *Thin Solid Films* **254**, 246 (1995).
29. R. G. Freeman *et al.*, *Science* **267**, 1629 (1995).
30. J. Schmitt *et al.*, *Adv. Mater.* **9**, 61 (1997).
31. S. W. Keller, H.-N. Kim, T. E. Mallouk, *J. Am. Chem. Soc.* **116**, 8817 (1994).
32. W. Kong *et al.*, *Makromol. Chem. Rapid Commun.* **15**, 405 (1994).
33. Y. Lvov, K. Ariga, T. Kunitake, *J. Am. Chem. Soc.* **117**, 6117 (1995).
34. E. R. Kleinfeld and G. S. Ferguson, *Science* **265**, 370 (1994).
35. G. S. Ferguson and E. R. Kleinfeld, *Adv. Mater.* **7**, 414 (1995).
36. E. R. Kleinfeld and G. S. Ferguson, *Chem. Mater.* **7**, 2327 (1995).
37. Y. Lvov, K. Ariga, I. Ichinose, T. Kunitake, *Langmuir* **12**, 3038 (1996).
38. Y. Lvov *et al.*, *ibid.* **10**, 4232 (1994).
39. D. L. Feldheim, K. C. Grabar, M. J. Natan, T. E. Mallouk, *J. Am. Chem. Soc.* **118**, 7640 (1996).
40. B. Philipp, H. Dautzenberg, K.-J. Linow, J. Kötz, W. Dawydoff, *Prog. Polym. Sci.* **14**, 91 (1989).
41. Z. Wang, T. Lan, T. J. Pinnavaia, *Chem. Mater.* **8**, 2200 (1996).
42. W. L. Ijdo, T. Lee, T. J. Pinnavaia, *Adv. Mater.* **8**, 79 (1996).
43. T. J. Pinnavaia, T. Lan, Z. Wang, H. Shi, P. D. Kaviratna, in *Nanotechnology: Molecularly Designed Materials*, vol. 622 of *ACS Symposium Series* (American Chemical Society, Washington, DC, 1996), pp. 250–261.
44. T. Lan and T. J. Pinnavaia, *Mater. Res. Soc. Symp. Proc.* **435**, 79 (1996).
45. R. Krishnamoorti, R. A. Vaia, E. P. Giannelis, *Chem. Mater.* **8**, 1728 (1996).
46. E. P. Giannelis, *Adv. Mater.* **8**, 29 (1996).
47. G. Decher and J. Schmitt, *Prog. Colloid Polym. Sci.* **89**, 160 (1992).
48. Y. Lvov, G. Decher, H. Möhwald, *Langmuir* **9**, 481 (1993).
49. H. Hong *et al.*, *Adv. Mater.* **7**, 846 (1995).
50. J. Schmitt *et al.*, *Macromolecules* **26**, 7058 (1993).
51. D. Korneev, Y. Lvov, G. Decher, J. Schmitt, S. Yaradaikin, *Physica B* **213–214**, 954 (1995).
52. G. Decher, Y. Lvov, J. Schmitt, *Thin Solid Films* **244**, 772 (1994).
53. H. Dautzenberg, J. Hartmann, S. Grunewald, F. Brand, *Ber. Bunsenges. Phys. Chem.* **100**, 1024 (1996).
54. W. Chen and T. J. McCarthy, *Macromolecules* **30**, 78 (1997).
55. M. Lösche, J. Schmitt, G. Decher, W. G. Bouwman, K. Kjær, in preparation.
56. F. Saremi, E. Maassen, B. Tieke, G. Jordan, W. Rammensee, *Langmuir* **11**, 1068 (1995).
57. G. J. Kellog *et al.*, *ibid.* **12**, 5109 (1996).
58. A. C. Fou and M. F. Rubner, *Macromolecules* **28**, 7115 (1995).
59. G. Decher, in *The Polymeric Materials Encyclopedia: Synthesis, Properties, and Applications*, J. C. Salamone, Ed. (CRC Press, Boca Raton, FL, 1996), vol. 6, 4540.
60. J.-D. Hong, K. Lowack, J. Schmitt, G. Decher, *Prog. Colloid Polym. Sci.* **93**, 98 (1993).
61. G. Decher, B. Lehr, K. Lowack, Y. Lvov, J. Schmitt, *Biosensors Bioelectronics* **9**, 677 (1994).
62. P.-G. He *et al.*, *Mater. Sci. Eng.* **C2**, 103 (1994).
63. P. T. Hammond and G. M. Whitesides, *Macromolecules* **28**, 7569 (1995).
64. T. G. Vargo *et al.*, *Supramol. Sci.* **2**, 169 (1996).
65. S. L. Clark, M. Montague, P. T. Hammond, *ibid.* **4**, 141 (1997).
66. W. B. Stockton and M. F. Rubner, *Macromolecules* **30**, 2717 (1997).
67. Y. Shimazaki, M. Mitsuishi, S. Ito, M. Yamamoto, *Langmuir* **13**, 1385 (1997).
68. G. Decher, *Nachr. Chem. Tech. Lab.* **41**, 793 (1993).
69. K. Chen, W. B. Caldwell, C. A. Mirkin, *J. Am. Chem. Soc.* **115**, 1193 (1993).
70. J. Schmitt, thesis, Johannes Gutenberg-Universität, Mainz, Germany (1996).
71. Y. Lvov, G. Decher, G. Sukhorukov, *Macromolecules* **26**, 5396 (1993).
72. G. B. Sukhorukov, H. Möhwald, G. Decher, Y. M. Lvov, *Thin Solid Films* **284–285**, 220 (1996).
73. Y. Lvov, K. Ariga, T. Kunitake, *Chem. Lett.* **1994**, 2323 (1994).
74. M. Gao *et al.*, *J. Chem. Soc. Chem. Commun.* **1994**, 2777 (1994).
75. N. A. Kotov, I. Dékány, J. H. Fendler, *J. Phys. Chem.* **99**, 13065 (1995).
76. ———, *Adv. Mater.* **8**, 637 (1996).
77. K. Ariga, Y. Lvov, M. Onda, I. Ichinose, T. Kunitake, *Chem. Lett.* **1997**, 125 (1997).
78. Y. Sun, X. Zhang, C. Sun, B. Wang, J. Shen, *Macromol. Chem. Phys.* **197**, 147 (1996).
79. M. Onda, Y. Lvov, K. Ariga, T. Kunitake, *Biotechnol. Bioeng.* **51**, 163 (1996).
80. ———, *J. Ferment. Bioeng.* **82**, 502 (1996).
81. R. von Klitzing and H. Möhwald, *Thin Solid Films* **284–285**, 352 (1996).
82. ———, *Macromolecules* **29**, 6901 (1996).
83. R. Pommersheim, J. Schrenzenmeir, W. Vogt, *Macromol. Chem. Phys.* **195**, 1557 (1994).
84. S. W. Keller, S. A. Johnson, E. S. Brigham, E. H. Yonemoto, T. E. Mallouk, *J. Am. Chem. Soc.* **117**, 12879 (1995).
85. X. Zhang, M. Gao, X. Kong, Y. Sun, J. Shen, *J. Chem. Soc. Chem. Commun.* **1994**, 1055 (1994).
86. T. M. Cooper, A. L. Campbell, R. L. Crane, *Langmuir* **11**, 2713 (1995).
87. A. Laschewsky *et al.*, *Thin Solid Films* **284–285**, 334 (1996).
88. J. K. Lee, D. S. Yoo, E. S. Handy, M. F. Rubner, *Appl. Phys. Lett.* **69**, 1686 (1996).
89. Y. Sun *et al.*, *J. Chem. Soc. Chem. Commun.* **1996**, 2379 (1996).
90. F. Saremi, G. Lange, B. Tieke, *Adv. Mater.* **8**, 923 (1996).
91. K. Ariga, Y. Lvov, T. Kunitake, *J. Am. Chem. Soc.* **119**, 2224 (1997).
92. P. Stroeve, V. Vasques, M. A. N. Coelho, J. F. Rabolt, *Thin Solid Films* **284–285**, 708 (1996).
93. M. Ferreira, M. F. Rubner, B. R. Hsieh, *Mater. Res. Soc. Symp. Proc.* **328**, 119 (1994).
94. J. Tian *et al.*, *Polym. Prepr. Am. Chem. Soc. Div. Polym. Chem.* **35**, 761 (1994).
95. A. C. Fou, O. Onitsuka, M. Ferreira, M. F. Rubner, B. R. Hsieh, *Mater. Res. Soc. Symp. Proc.* **369**, 575 (1995).
96. M. Onoda and K. Yoshino, *J. Appl. Phys.* **78**, 4456 (1995).
97. J. Tian *et al.*, *Adv. Mater.* **7**, 395 (1995).
98. J. Tian, C. C. Wu, M. E. Thompson, J. C. Sturm, R. A. Register, *Chem. Mater.* **7**, 2190 (1995).
99. A. C. Fou, O. Onitsuka, M. Ferreira, M. F. Rubner, B. R. Hsieh, *J. Appl. Phys.* **79**, 7501 (1996).
100. H. Hong *et al.*, *ibid.*, p. 3082.
101. B. Lehr, M. Seufert, G. Wenz, G. Decher, *Supramol. Sci.* **2**, 199 (1996).
102. O. Onitsuka, A. C. Fou, M. Ferreira, B. R. Hsieh, M. F. Rubner, *J. Appl. Phys.* **80**, 4067 (1996).
103. H. Hong *et al.*, *Supramol. Sci.* **4**, 67 (1997).
104. B. Lehr, J. Schmitt, R. Oeser, G. Decher, in preparation.
105. R. P. Feynman, in *Miniaturization*, H. D. Gilbert, Ed. (Reinhold, New York, 1961), pp. 282–296.

Computational Design of Hierarchically Structured Materials

G. B. Olson

A systems approach that integrates processing, structure, property, and performance relations has been used in the conceptual design of multilevel-structured materials. For high-performance alloy steels, numerical implementation of materials science principles provides a hierarchy of computational models defining subsystem design parameters that are integrated, through computational thermodynamics, in the comprehensive design of materials as interactive systems. Designed properties combine strength, toughness, and resistance to impurity embrittlement. The methods have also been applied to nonferrous metals, ceramics, and polymers.

For millennia, materials have been developed through the empirical correlation of processing and properties. The past century has seen the formation of a science of materials that has defined the structural basis of materials behavior, but its role has primarily been to explain the products of empiricism after their development. In the past decade, the numerical implementation of materials science principles and the integration of resulting computational capabilities within a systems engineering framework has given birth to a revolutionary approach (*1*) in the form of quantitative conceptual design of materials.

The author is in the Department of Materials Science and Engineering, Northwestern University, 2225 North Campus Drive, Evanston, IL 60208–3108, USA.